IET Microwaves, Antennas & Propagation

Research Article

IET Journals
The Institution of Engineering and Technology

Enhanced cognition-driven formulation of space mapping for equal-ripple optimisation of microwave filters

ISSN 1751-8725
Received on 7th April 2017
Accepted on 29th August 2017
E-First on 6th December 2017
doi: 10.1049/iet-map.2017.0238
www.ietdl.org

Chao Zhang[1], Feng Feng[1,2], Qi-Jun Zhang[1] ✉, John W. Bandler[3]

[1]*Department of Electronics, Carleton University, Ottawa, Canada*
[2]*School of Electronic Information Engineering, Tianjin University, Tianjin, People's Republic of China*
[3]*Department of Electrical and Computer Engineering, McMaster University, Hamilton, Canada*
✉ *E-mail: qjz@doe.carleton.ca*

Abstract: A recently introduced cognition-driven formulation of space mapping (SM) is an efficient method for equal-ripple optimisation of microwave filters. Feature frequency parameters and ripple height parameters are utilised. The technique requires the assumption that the initial number of feature parameters is correct, and uses an equally divided passband specification as a preliminary target. The present study proposes an enhanced technique which can correct the number of feature frequency parameters, thus it can work well even if the filter response of the initial point has an incorrect number of feature frequency parameters. Additionally, the enhanced technique incorporates filter design knowledge of the Chebyshev filter function into cognition-driven SM. The authors propose to use the feature frequency parameters of the Chebyshev filter function response curve to obtain the target for cognition-driven SM. A new trust region mechanism handles new parameters in the proposed process of correcting the number of feature frequency parameters and guarantees convergence. The technique is suitable for the design of filters with equal-ripple responses. It is illustrated by two microwave filter examples.

1 Introduction

Space mapping (SM) is nowadays an important methodology to address computational challenges in microwave design optimisation, such as electromagnetic (EM) optimisation [1, 2]. The SM concept takes advantage of the computational efficiency of coarse models and the accuracy of fine models [1]. Coarse models are typically empirical functions or equivalent circuits, which are computationally efficient but the accuracy is low. Fine models can be provided by an EM simulator, which is accurate, but computationally intensive. SM establishes a mathematical link between the coarse and fine models and directs the bulk of the central processing unit-intensive computations to the coarse models while preserving the accuracy of the fine models [2]. Recent progress has focused on several areas, such as aggressive SM [2], a cognition driven formulation of SM [3], portable SM for efficient modelling [4], output SM [5], tuning SM [6], zero-pole SM [7], parallel SM [8] and dynamic neuro-SM [9].

A further development in SM is to address the situation where equivalent circuit coarse models are not available. In [10], to build a coarse model for waveguide filters, a small number of accessible modes in the method of moments are considered to obtain a faster simulation at the expense of solution accuracy. In [11, 12], coarse mesh EM simulations are used as coarse models. Sensitivity information from EM simulations has been used to increase the effectiveness of SM with EM-based coarse models [12].

Several other recent works have investigated the possible feature parameters in model responses. Zeros and poles of filter transfer functions are used as feature parameters for optimisation and filter tuning in [7, 13]. In [14, 15], the feature parameters of filter responses are used for design optimisation and statistical analysis of microwave structures. In [16], the response features are utilised to develop variable-fidelity feature-based modelling. The cognition-driven formulation of SM in [3] uses two sets of intermediate feature space parameters to increase the optimisation efficiency and the ability to avoid being trapped in local minima. This technique also addresses the challenge of SM when explicit equivalent circuit coarse models are not available. It assumes that the number of feature frequency parameters is correct, and uses an equally divided passband specification as a preliminary target to simplify the formulation. This technique in [3] can address most of the cases, where engineers can obtain a Chebyshev response with a correct number of feature frequency parameters at the initial design. However, in some situations, it is not easy to determine the proper EM geometry to achieve the ideal Chebyshev response before optimisation. In these situations, the initial design may not be close to the optimal solution, and the number of feature frequency parameters of the starting point may even be incorrect.

The present study is a major advance over [3]. We propose an enhanced cognition-driven SM technique that can work well even if the number of feature frequency parameters is not correct. Our proposed enhanced cognition-driven SM can correct the number of feature frequency parameters so that the cognition-driven SM in [3] can still be applied. Furthermore, in filter design, the feature frequency parameters of the optimal solution are not uniformly distributed. The proposed technique incorporates filter design knowledge of the Chebyshev filter function into our cognition-driven SM to further increase the efficiency and effectiveness of optimisation. We propose to use the feature frequency parameters of the Chebyshev filter function response curve to obtain the target for our enhanced cognition-driven SM method. A new trust region mechanism is formulated to handle new parameters in the proposed process of correcting the number of feature frequency parameters and to guarantee convergence.

2 Proposed algorithm to correct the number of feature frequency parameters

2.1 Summary of the existing cognition-driven SM method [3]

For an equal-ripple bandpass filter, the filter response curve (e.g. $|S_{11}|$ versus frequency) has several minima which are referred to as feature frequency parameters. Let $\boldsymbol{f}$ represent a vector of such feature frequency parameters. The maximum values of $|S_{11}|$ (in dB) between these feature frequency points are also important features of the response curve and are represented by ripple height parameters. We use vector $\boldsymbol{t}$ to represent them.

Let $\boldsymbol{x}$ represent the physical/geometrical design variables. The cognition-driven SM optimisation method has two stages. In the first stage, we perform SM between $\boldsymbol{x}$ (i.e. the original optimisation

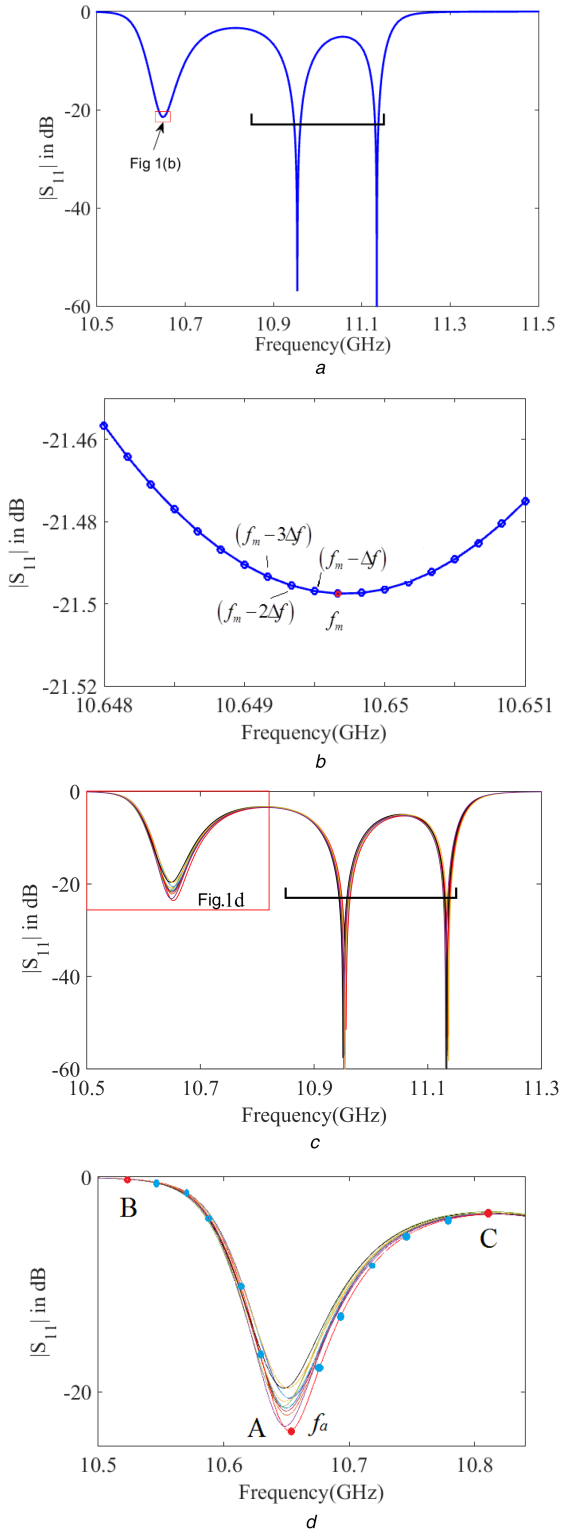

Fig. 1 *Four-pole waveguide filter*

(a) Initial point of a four-pole waveguide filter with an incorrect number of feature frequency parameters. The correct number of feature frequency parameters for the four-pole waveguide filter response should be four, while this response curve has only three, ***(b)*** Detailed information near one feature frequency. We calculate the left slope of feature frequency f_m using the *S*-parameters at frequency samples f_m, $(f_m-\Delta f)$, $(f_m-2\Delta f)$, and $(f_m-3\Delta f)$, ***(c)*** $2N+1$ response curves generated with the star distribution in parallel, ***(d)*** Detailed information near the ambiguous feature (Point A). Point B is located on the response curve where the *S*-parameter is −1 dB. Point C is located on the response curve where *S*-parameter is at a maximum between two feature frequency parameters

variables) and the feature frequency parameters $\boldsymbol{f}$. The mapping from design variables to feature frequency parameters is used to move all the feature frequency parameters into the design specification passband by changing the design variables according to a uniformly distributed target as follows:

$$\boldsymbol{f}_{\mathrm{d}} = \left[f_{\mathrm{L}} \quad f_{\mathrm{L}}+\frac{f_{\mathrm{H}}-f_{\mathrm{L}}}{M-1} \quad \cdots \quad f_{\mathrm{L}}+\frac{f_{\mathrm{H}}-f_{\mathrm{L}}}{M-1}(M-2) \quad f_{\mathrm{H}}\right]^{\mathrm{T}}, \tag{1}$$

where $\boldsymbol{f}_{\mathrm{d}}$ is the desired set of feature frequency parameters in the first stage. M represents the number of poles of the filter. f_{L} and f_{H} denote the lower and higher frequency edges of the filter passband, respectively. In the second stage, the mapping from feature frequency parameters $\boldsymbol{f}$ to ripple height parameters $\boldsymbol{t}$ is obtained. Using the mappings from $\boldsymbol{x}$ space to $\boldsymbol{f}$ space and from $\boldsymbol{f}$ space to $\boldsymbol{t}$ space, our method can minimise the variance of all the ripple height parameters by changing the design variables. In (1), the method requires the assumption that the number of feature frequency parameters should be equal to the number of poles M.

2.2 Proposed method to find the ambiguous feature

For the cognition-driven SM optimisation method, a major remaining challenge is when the number of feature frequency parameters at the initial point is not equal to the number of poles, as shown in Fig. 1*a*. The correct number of feature frequency parameters for a four-pole waveguide filter response should be four, while the response curve shown in Fig. 1*a* has only three. This will give the target defined in (1) incomplete information, which will make it difficult for the cognition-driven SM [3] to proceed in the first stage. Therefore, we propose a new method to address this situation.

In the optimised filter design, feature frequency parameters should be spaced apart, and the *S*-parameter response curve at each feature frequency should behave as a sharp valley. Before such a solution is found, some feature frequency parameters may be close to each other to show only one minimum in the response curve [13]. Two or more feature frequency parameters may combine to produce only one valley in the filter response. Furthermore, based on empirical observation we can find that the valley at that minimum is smooth rather than sharp. Following our definition of feature frequency parameters, we will still consider this minimum as a single feature frequency parameter (even though it actually represents one or more feature frequency parameters). In this study, we call such a feature an ambiguous feature.

In the proposed technique, we first identify the ambiguous feature frequency and then use derivative information of the response curve to guide the correction of the number of feature frequency parameters iteratively. Since this new process cannot be guaranteed to converge by the trust region method used in the previous technique [3], we further propose to add a new trust region mechanism. This new trust region method is formulated to address the new requirement of processing the ambiguous feature in the proposed enhanced method.

Let $\boldsymbol{x}^{(k)}$ be the current solution of $\boldsymbol{x}$ in the kth iteration, where k represents the iteration number in the optimisation process. We generate multiple sample points with a star distribution around $\boldsymbol{x}^{(k)}$ in the kth iteration. We perturb $\boldsymbol{x}^{(k)}$ twice along each dimension, once towards the positive direction and once towards the negative direction. In this way, we find $2N$ sample points, where N is the number of design variables. Let $\boldsymbol{R}(\boldsymbol{x}_i, \omega)$ denote the response corresponding to a vector of design variables $\boldsymbol{x}_i$ at frequency ω and the ith point in the star distribution, $i = 1, 2, \ldots, 2N+1$. We perform EM simulations at all the $2N+1$ data points to obtain the responses $\boldsymbol{R}(\boldsymbol{x}_i, \omega)$ at $\boldsymbol{x}_i$, using $2N+1$ processors in parallel [8]. Fig. 1*c* shows typical response curves of $2N+1$ points generated with star distribution. The algorithm uses parallel computation to perform the $2N+1$ EM simulations simultaneously, therefore the total computation time for the $2N+1$ EM simulations is similar to (or only incrementally more than) that of a single EM simulation.

We can obtain the feature frequency parameters $\boldsymbol{f}^{(k)}$ at $\boldsymbol{x}^{(k)}$ as follows:

$$\boldsymbol{f}^{(k)} = \begin{bmatrix} f_1 & f_2 & \cdots & f_{M'} \end{bmatrix}^{\mathrm{T}} \tag{2}$$

where M' represents the present number of feature frequency parameters in the current iteration. If M' is not equal to M, we should correct the number of feature frequency parameters by changing the values of design variables $\boldsymbol{x}$ such that M' becomes equal to M. To find the ambiguous feature, here we introduce a new concept which defines the sharpness of the feature frequency parameters. Let V_{f_m} be defined as the sharpness parameter of a feature frequency f_m, where f_m represents the mth feature frequency parameter for $m = 1, 2, \ldots, M'$. Let Δf be defined as the frequency step in the simulated response curve. We obtain three closest frequency samples $(f_m - \Delta f)$, $(f_m - 2\Delta f)$, and $(f_m - 3\Delta f)$ on the left side of feature frequency f_m, which are shown in Fig. 1*b*. Let $\boldsymbol{v}$ be defined as a frequency vector which contains those four frequency samples, i.e. $\boldsymbol{v} = \begin{bmatrix} f_m & (f_m - \Delta f) & (f_m - 2\Delta f) & (f_m - 3\Delta f) \end{bmatrix}^{\mathrm{T}}$. Let $\boldsymbol{u}$ be defined as a vector which contains the *S*-parameters of those four frequency samples in $\boldsymbol{v}$. We use a linear fit method to find a linear function

$$\boldsymbol{u} = \alpha + \beta \boldsymbol{v}, \tag{3}$$

where α and β represent the coefficients of the linear function which can be analytically solved.

Let $\beta^{\mathrm{l}}_{f_m}$ and $\beta^{\mathrm{r}}_{f_m}$ be defined as the left slope and right slope of the feature frequency parameter f_m, respectively. The left slope $\beta^{\mathrm{l}}_{f_m}$ of a feature frequency parameter f_m is determined by

$$\beta^{\mathrm{l}}_{f_m} = \beta \tag{4}$$

Similarly, we can obtain the right slope $\beta^{\mathrm{r}}_{f_m}$ of the feature frequency parameter f_m, using three closest frequency samples on the right side of feature frequency parameter f_m.

Here we define the sharpness parameter V_{f_m} of a feature frequency parameter f_m as

$$V_{f_m} = \left|\beta^{l}_{f_m}\right| + \left|\beta^{r}_{f_m}\right|, \quad \forall m = 1, 2, \ldots, M'. \tag{5}$$

We can find the ambiguous feature frequency f_{a}, which has the lowest sharpness parameter value among that of all the feature frequency parameters

$$V_{f_{\mathrm{a}}} = \min \{V_{f_1}, V_{f_2}, \ldots, V_{f_{M'}}\}. \tag{6}$$

2.3 Proposed method to split the ambiguous feature according to the derivative information of the response curve

After finding the ambiguous feature, we try to obtain derivative information around it to split it into multiple feature frequency parameters by adjusting the values of the design variables. Here we distinguish between two types of curves near the ambiguous feature frequency, which are curve AB and curve AC shown in Fig. 1*d*. Point A represents the ambiguous feature point, where the ambiguous feature frequency f_{a} is obtained by (6). Point B is located on the response curve where the *S*-parameter is −1 dB. Point C is located on the response curve where the *S*-parameter is at maximum between two feature frequency parameters. Let f_{b} and f_{c} be the frequencies at point B and point C, respectively.

In reality, there are three different cases for the location of the ambiguous feature. In the first case, the ambiguous feature is the smallest among all the feature frequency parameters. Second, the ambiguous feature is located between other feature frequency parameters. In the third case, the ambiguous feature is the largest among all the feature frequency parameters. The curve types near the ambiguous feature in the first case are curve BA and AC, which are shown in Fig. 1*d*. The curve types near the ambiguous feature in the second case are curve CA and AC. The curve types in the third case will be curve CA and AB.

We further formulate a quantitative description of the response curves near the ambiguous feature. Let β_{L} and β_{R} be defined as the slopes of curve BA and curve AC. For the example shown in Fig. 1*d*, we divide the frequency range between A and B of the response curve into six equal parts. We pick three frequency points $(f_{\mathrm{a}} - ((f_{\mathrm{a}} - f_{\mathrm{b}})/6))$, $(f_{\mathrm{a}} - ((f_{\mathrm{a}} - f_{\mathrm{b}})/3))$ and $(f_{\mathrm{a}} - ((f_{\mathrm{a}} - f_{\mathrm{b}})/2))$ that are close to the ambiguous feature frequency on curve BA. We also obtain the *S*-parameters at those three frequency points and f_{a}. Then the slope β_{L} of curve BA can be obtained by the linear fit method (3) and (4). Similarly, we obtain three more frequency points $(f_{\mathrm{a}} + ((f_{\mathrm{c}} - f_{\mathrm{a}})/6))$, $(f_{\mathrm{a}} + ((f_{\mathrm{c}} - f_{\mathrm{a}})/3))$ and $(f_{\mathrm{a}} + ((f_{\mathrm{c}} - f_{\mathrm{a}})/2))$ that are close to the ambiguous feature frequency on curve AC. The slope β_{R} of the curve AC on the right side of the ambiguous feature can be obtained.

The basic idea for splitting the ambiguous feature frequency is to adjust design variables $\boldsymbol{x}$ to increase the absolute value of β_{L} and β_{R}. As shown in Fig. 1*d*, when the design variables change, the slopes β_{L} and β_{R} vary. We want to build a mapping from the slopes β_{L} and β_{R} to the design variables $\boldsymbol{x}$. Let $\boldsymbol{J}_1$ represent the mapping matrix from slopes β_{L} and β_{R} to the design parameters $\boldsymbol{x}$. Using the $2N + 1$ EM data, we can obtain $\boldsymbol{J}_1$ as follows:

$$\boldsymbol{J}_1 = \left(\frac{\partial [\beta_{\mathrm{L}} \quad \beta_{\mathrm{R}}]}{\partial \boldsymbol{x}}\right)^{\mathrm{T}} \tag{7}$$

Let $\beta^{(k)}_{\mathrm{L}}$ and $\beta^{(k)}_{\mathrm{R}}$ represent the slopes β_{L} and β_{R} in the kth iteration. Once the mapping $\boldsymbol{J}_1$ is built, we can increase the absolute values of the slopes by changing the design variables $\boldsymbol{x}^{(k)}$ in the kth iteration, so that the ambiguous feature will be split. Here we define an error function as

$$E_1(\boldsymbol{s}) = g([\boldsymbol{J}_1^{(k)}\boldsymbol{s}]_{1,1}, 2\beta^{(k)}_{\mathrm{L}}) + g([\boldsymbol{J}_1^{(k)}\boldsymbol{s}]_{2,1}, 2\beta^{(k)}_{\mathrm{R}}), \tag{8}$$

where $\boldsymbol{s}$ is the prospective change of design variables $\boldsymbol{x}$ in the optimisation process, and function g with two real inputs p and q is defined as

$$g(p, q) = \begin{cases} |p - q|, & \text{if } |p| \leqslant |q| \\ 0, & \text{else} \end{cases} \tag{9}$$

and $\boldsymbol{J}_1^{(k)}$ is the mapping matrix $\boldsymbol{J}_1$ in the kth iteration. By minimising E_1 in (8), we aim to increase the absolute values of the slopes $\beta^{(k)}_{\mathrm{L}}$ and $\beta^{(k)}_{\mathrm{R}}$. In our practice, we set our goal such that this increase is by a factor of at least 2, as implied in (8).

At the same time, we want to fix the locations of the non-ambiguous feature frequency parameters to prevent them from moving together to form another ambiguous feature. Therefore, we also consider the mapping from the non-ambiguous feature frequency parameters to the design variables. Let $\boldsymbol{J}_2$ represent the mapping matrix from the non-ambiguous feature frequency parameters to the design parameters $\boldsymbol{x}$. Using $2N + 1$ EM data, we can calculate $\boldsymbol{J}_2$ as follows:

$$\boldsymbol{J}_2 = \left(\frac{\partial \boldsymbol{f}'^{\mathrm{T}}}{\partial \boldsymbol{x}}\right)^{\mathrm{T}}, \tag{10}$$

where $\boldsymbol{f}'$ represents a vector of the non-ambiguous feature frequency parameters.

To keep the locations of the non-ambiguous feature frequency parameters fixed, we define a new error function as

$$E_2(\boldsymbol{s}) = \| \boldsymbol{J}_2^{(k)}\boldsymbol{s} \|, \tag{11}$$

where $\boldsymbol{J}_2^{(k)}$ is the mapping matrix $\boldsymbol{J}_2$ in the kth iteration. E_2 aims at fixing the locations of non-ambiguous feature frequency parameters.

Subsequently, we can solve for the change $\boldsymbol{s}^{(k)}$ in the kth iteration by

$$\boldsymbol{s}^{(k)} = \arg \min_{\| s \| \leqslant \delta^{(k)}} (E_1(\boldsymbol{s}) + \lambda E_2(\boldsymbol{s})), \tag{12}$$

where $\delta^{(k)}$ is the trust radius and $\boldsymbol{s}^{(k)}$ is the prospective change of design variables $\boldsymbol{x}$ in the kth iteration. λ is a weighting factor, which is used to provide a balance between the importance of fixing the locations of the feature frequency parameters and increasing the values of the slopes β_{L} and β_{R}.

2.4 Trust region method for splitting the ambiguous feature

The trust region method described in the previous cognition-driven SM method [3] does not work here, because of the new procedure of changing the number of feature frequency parameters. Here we define a new specific trust region method to guarantee a consistent increase in the slopes so that the ambiguous feature can be split.

Once $\boldsymbol{s}^{(k)}$ is determined, we perform $2N+1$ EM simulations using the star distribution in parallel around the new centre $(\boldsymbol{x}^{(k)} + \boldsymbol{s}^{(k)})$; subsequently, we can obtain $f|_{(\boldsymbol{x}^{(k)} + \boldsymbol{s}^{(k)})}$, which represents the feature frequency parameters at $(\boldsymbol{x}^{(k)} + \boldsymbol{s}^{(k)})$. The stopping criterion is that the number of feature frequency parameters increases, and this means the ambiguous feature is split.

If the number of feature frequency parameters remains the same, we calculate the slopes β_{L} and β_{R} at $(\boldsymbol{x}^{(k)} + \boldsymbol{s}^{(k)})$. For convenience, we let β_{L}^s and β_{R}^s represent the β_{L} and β_{R} at $(\boldsymbol{x}^{(k)} + \boldsymbol{s}^{(k)})$.

We calculate the adjustment index r for the trust radius according to the changes of slopes at $(\boldsymbol{x}^{(k)} + \boldsymbol{s}^{(k)})$

$$r = \frac{U(\beta_{\mathrm{L}}^{(k)}, \beta_{\mathrm{R}}^{(k)}) - U(\beta_{\mathrm{L}}^s, \beta_{\mathrm{R}}^s)}{U(\beta_{\mathrm{L}}^{(k)}, \beta_{\mathrm{R}}^{(k)}) - U(\beta_{\mathrm{L}}^{(k)} + [\boldsymbol{J}_1^{(k)}\boldsymbol{s}^{(k)}]_{1,1}, \beta_{\mathrm{R}}^{(k)} + [\boldsymbol{J}_1^{(k)}\boldsymbol{s}^{(k)}]_{2,1})}, \tag{13}$$

where U is the objective function with two inputs z_1 and z_2 defined as

$$U(z_1, z_2) = g(z_1, 2\beta_{\mathrm{L}}^{(k)}) + g(z_2, 2\beta_{\mathrm{R}}^{(k)}). \tag{14}$$

If the number of feature frequency parameters remains the same, and the following condition

$$U(\beta_{\mathrm{L}}^s, \beta_{\mathrm{R}}^s) \leqslant U(\beta_{\mathrm{L}}^{(k)}, \beta_{\mathrm{R}}^{(k)}) \tag{15}$$

is satisfied, we accept the step $\boldsymbol{s}^{(k)}$ and update the design variables as

$$\boldsymbol{x}^{(k+1)} = \boldsymbol{x}^{(k)} + \boldsymbol{s}^{(k)} \tag{16}$$

At the same time, we should update the radius of the trust region using the following equation [17]:

$$\delta^{(k+1)} = \begin{cases} 0.618\| \boldsymbol{s}^{(k)} \|, & \text{if } r < 0.1, \\ \min\left\{1.214\delta^{(k)}, \Delta^*\right\}, & \text{if } r > 0.8, \\ \| \boldsymbol{s}^{(k)} \|, & \text{otherwise}, \end{cases} \tag{17}$$

where Δ^* is the maximum value of the trust radius.

If (15) is not satisfied, $\boldsymbol{x}^{(k)}$ will be kept unchanged, and a new $\boldsymbol{s}^{(k)}$ is calculated by solving (12) with the updated trust radius $\delta^{(k)} = \delta^{(k+1)}$. Once the ambiguous feature is split (i.e. the number of feature frequency parameters increases), the algorithm stops. To make our proposed method more robust, we terminate the algorithm if one of the following conditions is satisfied: $\| \boldsymbol{x}^{(k+1)} - \boldsymbol{x}^{(k)} \| < 10^{-2}$ or $\delta^{(k+1)} < 10^{-3}$ [18].

2.5 Discussion

The process from (2) to (17) splits one ambiguous feature. After the process is finished, if the number of the feature frequency parameters is still not equal to the number of poles M, the process from (2)–(17) should be repeated until we obtain the correct number of feature frequency parameters.

In this study, our proposed method can determine the ambiguous feature parameters using (3)–(6), when two overlapping poles of the transfer function are relatively far from the imaginary frequency axis. When two poles are in the complex plane and close to the frequency axis, the sharpness parameter value of ambiguous feature parameter may be comparable with that of non-ambiguous feature parameters. In this situation, the method followed in this study may not be effective. This may be a direction of future research.

There are various types of filters with different transfer functions, such as bandpass, lowpass or highpass filters with Chebyshev, Elliptic, Butterworth, or Chained transfer functions. In this study, we focus on the challenges for designing bandpass filters with Chebyshev and Elliptic transfer functions. Designing other types of filters, where preserving precise locations for transmission zeros is important, is equally important and a heavy task. The technique followed in this study may not be effective. This is a possible direction for future research.

3 Chebyshev filter response target for the first stage of enhanced cognition-driven SM

Another improvement of the cognition-driven SM method is to incorporate more specific filter design knowledge into the formation to further enhance optimisation.

In the cognition-driven SM technique [3], the passband specified for the filter is divided into $(M-1)$ equal parts and the desired feature frequency parameters in the first stage are uniformly distributed. This equally divided target for the first stage simplifies the formulation. However, the feature frequency parameters of an optimal filter solution do not follow a uniform distribution unless the number of feature frequency parameters is equal to 3.

In this study, we use the Chebyshev filter equation [19] to model the real filter response and propose to use the feature frequency parameters of the Chebyshev filter response as the target feature frequency parameters for the first stage of cognition-driven SM.

We can obtain the Chebyshev filter transfer function using the order number M and design specifications. Later we find the feature frequency parameters of this Chebyshev filter response by solving

$$|H(\mathrm{j}\omega)| = 1 \tag{18}$$

A comparison between the uniformly distributed target and that obtained by the Chebyshev function is shown in Figs. 2*b* and 3*b*. Fig. 4 shows the flowchart of our enhanced cognition-driven SM technique.

4 Examples

4.1 Optimisation of a four-pole waveguide filter

The first example under consideration is a four-pole waveguide filter [10]. The tuning elements are penetrating posts of square cross-section placed at the centre of each cavity and each coupling window, as shown in Fig. 2*a*. h_1, h_2 and h_3 are the heights of the posts in the coupling windows, and $h_{\mathrm{c}1}$, $h_{\mathrm{c}2}$ are the heights of the posts in the resonant cavities. The design variables are $x = [h_1 \quad h_2 \quad h_3 \quad h_{\mathrm{c}1} \quad h_{\mathrm{c}2}]^{\mathrm{T}}$.

In our work, the EM evaluation is performed by the *ANSYS HFSS* EM simulator using the fast simulation feature. The desired

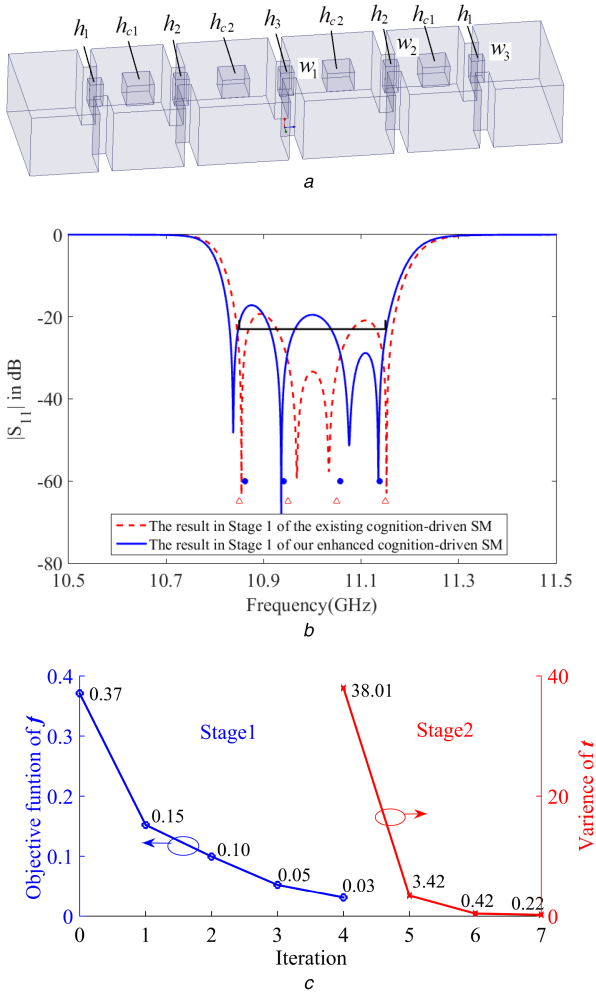

Fig. 2 *Figures for Example 1*

(a) Structure of the four-pole waveguide filter with design variables $x = [h_1 \quad h_2 \quad h_3 \quad h_{c1} \quad h_{c2}]^T$ and the implicit coarse and fine mesh SM parameters w_1, w_2 and w_3, ***(b)*** Results in Stage 1 of the existing cognition-driven SM method and our proposed technique for the four-pole waveguide filter in Case I. Round dots (•) represent the target obtained by the Chebyshev function in the proposed technique, and the triangles (Δ) represent the uniformly distributed target in the existing cognition-driven SM method, ***(c)*** Feature space objective functions for the four-pole waveguide filter example in Case II. In Stage 1, the objective function of $\boldsymbol{f}$ represents the error between the feature frequency parameters and the target. In Stage 2, the objective function represents the variance of ripple height parameters $\boldsymbol{t}$

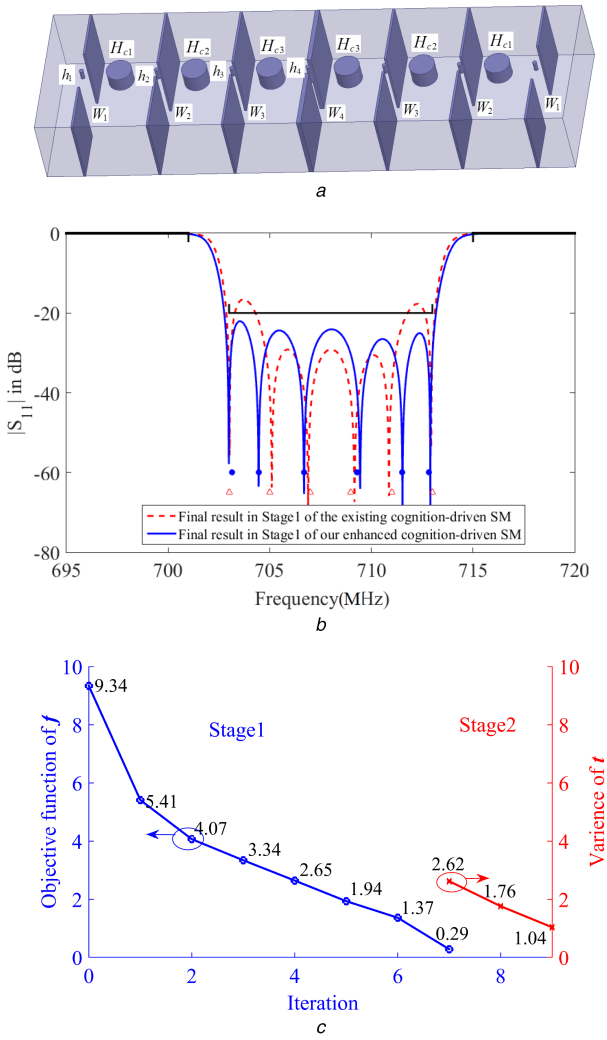

Fig. 3 *Figures for Example 2*

(a) Structure of the iris coupled cavity filter with design variables $\boldsymbol{x} = [W_1 \quad W_2 \quad W_3 \quad W_4 \quad H_{c1} \quad H_{c2} \quad H_{c3}]^T$ and the implicit coarse and fine mesh SM variables h_1, h_2, h_3 and h_4, ***(b)*** Results in Stage 1 of the existing cognition-driven SM method and our proposed technique for the iris coupled cavity filter in Case I. Round dots (•) represent the target obtained by the Chebyshev function and triangles (Δ) represent the uniformly distributed target in the existing cognition-driven SM method. The result in Stage 1 of our proposed enhanced technique produces a much better starting point for Stage 2, ***(c)*** Feature space objective functions for the iris coupled cavity filter examples. In Stage 1, the objective function of $\boldsymbol{f}$ represents the error between the feature frequency parameters and the target. In Stage 2, the objective function represents the variance of ripple height parameters $\boldsymbol{t}$

filter response has been chosen to be standard four-pole Chebyshev curve of 300-MHz bandwidth, $|S_{11}| \leqslant -23$ dB, and centred at 11 GHz.

There are two different cases for the number of feature frequency parameters of the filter response at the starting point. In Case I, we use a starting point with the correct number of feature frequency parameters, i.e., $M' = M = 4$. We use both the existing cognition-driven SM and our new enhanced technique to optimise this filter. For comparison, we use coarse and fine mesh SM and direct EM optimisation to optimise this filter. The comparison results are shown in Table 1. From the table, we can find both the existing cognition-driven SM method and the proposed enhanced technique work well. Since the feature frequency parameters of the Chebyshev filter response are used as the target in Stage 1 of our proposed technique, the result in Stage 1 of our proposed technique produces a better starting point for Stage 2, shown in Fig. 2*b*. However, both the direct EM optimisation method and coarse and fine mesh SM are trapped in a local minimum.

In Case II, the number of feature frequency parameters at the starting point is incorrect. The starting point is $\boldsymbol{x}^{(0)} = [3.030 \quad 4.670 \quad 4.304 \quad 3.490 \quad 3.018]^T$ (all values in mm). The response curve of the starting point has only three feature frequency parameters as shown in Fig. 5*a*. This incorrect number of feature frequency parameters will give the target defined in (1) incomplete information, which will make it difficult for the existing cognition-driven SM [3] to proceed in the first stage. Therefore, our proposed technique is needed. At the beginning of the optimisation, our algorithm can find that the first feature frequency parameter is the ambiguous feature. The sharpness parameters of those three feature frequency points are 8.831, 4.926×10^4 and 9.578×10^4, respectively. We can find that the sharpness parameter of the ambiguous feature is obviously smaller than that of non-ambiguous feature frequency parameters. After finding the ambiguous feature, we use our technique to split the ambiguous feature. Using our proposed technique, the solution with four feature frequency parameters is obtained after one iteration (8 min). The responses of the initial point and the first iteration are shown in Fig. 5*a*. From the figure, we can find that our algorithm can split the ambiguous feature while the locations of non-ambiguous feature frequency parameters are almost unchanged.

For comparison purposes, we use implicit coarse and fine mesh SM and direct EM optimisation to optimise this filter until the

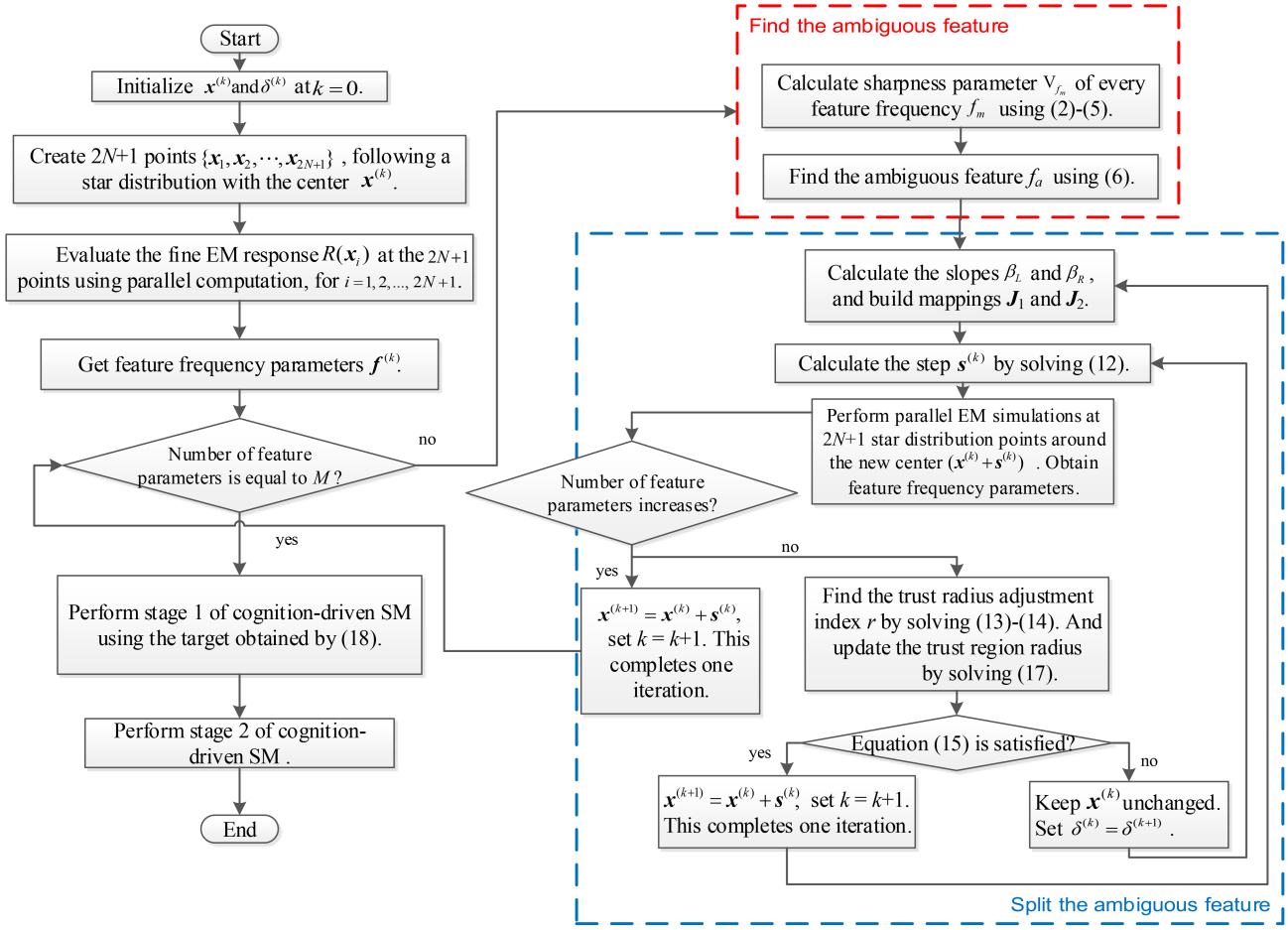

Fig. 4 *Flowchart of the enhanced cognition-driven SM technique*

Table 1 Comparisons of four optimisation methods for the four-pole waveguide filter example with correct number of feature frequency parameters at the initial filter in Case I

Optimisation method	Direct EM optimisation (existing technique)	Coarse/ fine mesh SM (existing technique)	Cognition-driven SM (existing technique)	Enhanced cognition SM (proposed technique)
no. of iterations	660	4	8	7
fine model evaluation time	660 × 4 min	5 × 4 min	(9 + 6[a]) × 6 min	(8 + 6[a]) × 6 min
training time	—	3 × 1 h	8 × 1 min	7 × 1 min
design optimisation time	—	4 × 1 h	8 × 1 min	7 × 1 min
total time	44 h	7 h 20 min	1 h 46 min	1 h 40 min
final value of objective function	25.42 (being trapped in local minimum)	98.21 (being trapped in local minimum)	− 0.06	− 0.02

[a]The number of EM simulations, which are not accepted during the trust region adjustment.

ambiguous feature is split. Fig. 5*b* shows that implicit coarse and fine mesh SM splits the ambiguous feature in one iteration, and takes more than 2 h in order to finish one SM iteration. The computation time is mostly spent on coarse mesh EM optimisations. Fig. 5*c* shows that direct EM optimisation achieves our goal to split the ambiguous feature into six iterations and that it takes nearly half an hour. We can find that our enhanced cognition-driven SM technique can quickly split the ambiguous feature to produce a good result with the correct number of feature frequency parameters.

After obtaining a solution with the correct number of feature frequency parameters, we use our enhanced technique to continue the optimisation. We can obtain the Chebyshev filter transfer function with the order number 4 and design specifications using the *cheby1* function in *Matlab*. The feature frequency parameters of the Chebyshev filter response are obtained using (18) and then used as the target at Stage 1 of our proposed technique. The optimal solution $x^{(7)} = [3.407 \quad 4.083 \quad 3.571 \quad 3.295 \quad 2.978]^T$ (all values in mm) is obtained after seven iterations, which include four iterations in Stage 1 and three iterations in Stage 2. Fig. 6*a* shows the result of Stage 1. The final result of our proposed method is shown in Fig. 6*b*. All the feature space objective functions [3] are shown in Fig. 2*c*.

For comparison purposes, we use implicit coarse and fine mesh SM to optimise this filter with the same starting point and the same specifications as those shown in Fig. 5*a*. The result is shown in Fig. 6*c*. The direct EM optimisation is also performed for additional comparison and the result shown in Fig. 6*d*. The results in Fig. 6 and Table 2 show that both implicit coarse and fine mesh SM and direct EM optimisation fall into local minima. The existing cognition-driven SM method cannot work well when the number of feature frequency parameters is not correct at the initial point. Our enhanced method can solve the initial point with an incorrect number of feature frequency parameters and achieves a better result within less time.

4.2 Optimisation of an iris coupled cavity filter

Consider the iris coupled cavity microwave bandpass filter shown in Fig. 3*a* [3]. The heights of the big cylinders H_{c1}, H_{c2}, and H_{c3} positioned at the cavity centres are responsible for tuning the frequencies in the cavity. The required coupling bandwidths are accomplished via the iris widths W_1, W_2, W_3, and W_4 for a pre-

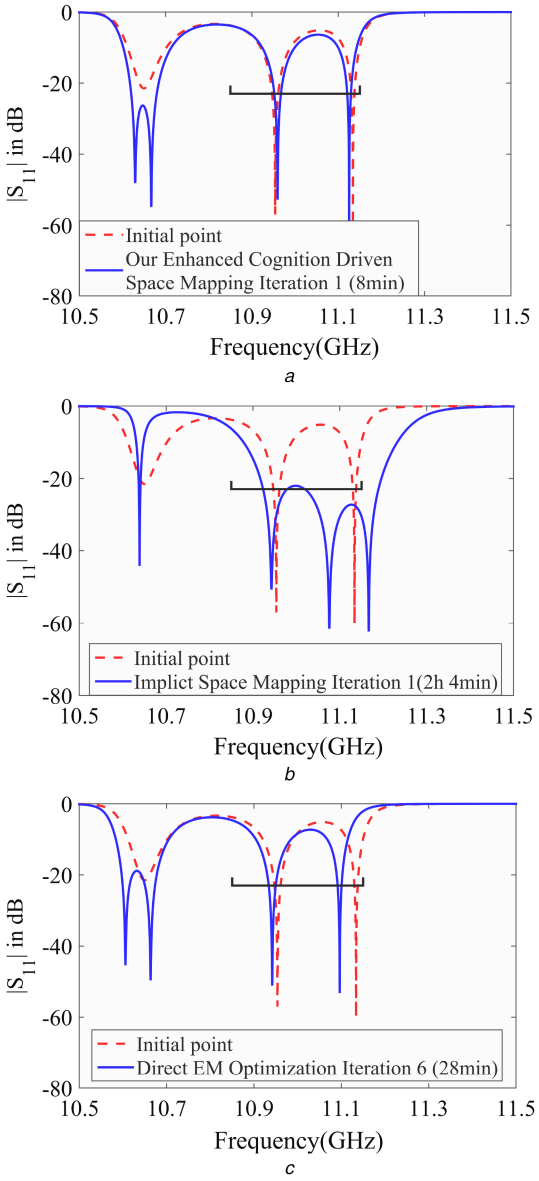

Fig. 5 *Different methods to split the ambiguous feature for the four-pole waveguide filter in Case II*

(a) Our enhanced cognition-driven SM method takes one iteration (8 min), ***(b)*** Implicit coarse and fine mesh SM takes one iteration (2 h 4 min), ***(c)*** Direct EM optimisation takes six iterations (28 min)

tuning. The design variables are $\boldsymbol{x} = [W_1 \quad W_2 \quad W_3 \quad W_4 \quad H_{c1} \quad H_{c2} \quad H_{c3}]^T$.

We provide the design specifications $|S_{11}| \leqslant -20$ dB in the frequency range 703–713 MHz, and $|S_{21}| \leqslant -10$ dB in the frequency ranges 690–701 and 715–720 MHz.

There are two different cases for the number of feature frequency parameters at the starting point. In Case I, we use a starting point with the correct number of feature frequency parameters, i.e. $M' = M = 6$. We use both the existing cognition-driven SM and our proposed enhanced technique to optimise this filter. For comparison, we also use coarse and fine mesh SM and direct EM optimisation to optimise this filter. The comparison results are shown in Table 3. From the table, we find that both the existing cognition-driven SM method and the proposed enhanced technique work well. Since the feature frequency parameters of the Chebyshev filter response are used as the target at Stage 1 of our proposed technique, the result in Stage 1 of our proposed enhanced technique produces a better starting point for Stage 2, shown in Fig. 3*b*. However, both direct EM optimisation and coarse and fine mesh SM are trapped in local minima.

In Case II, the number of feature frequency parameters at the starting point is incorrect. The starting point is

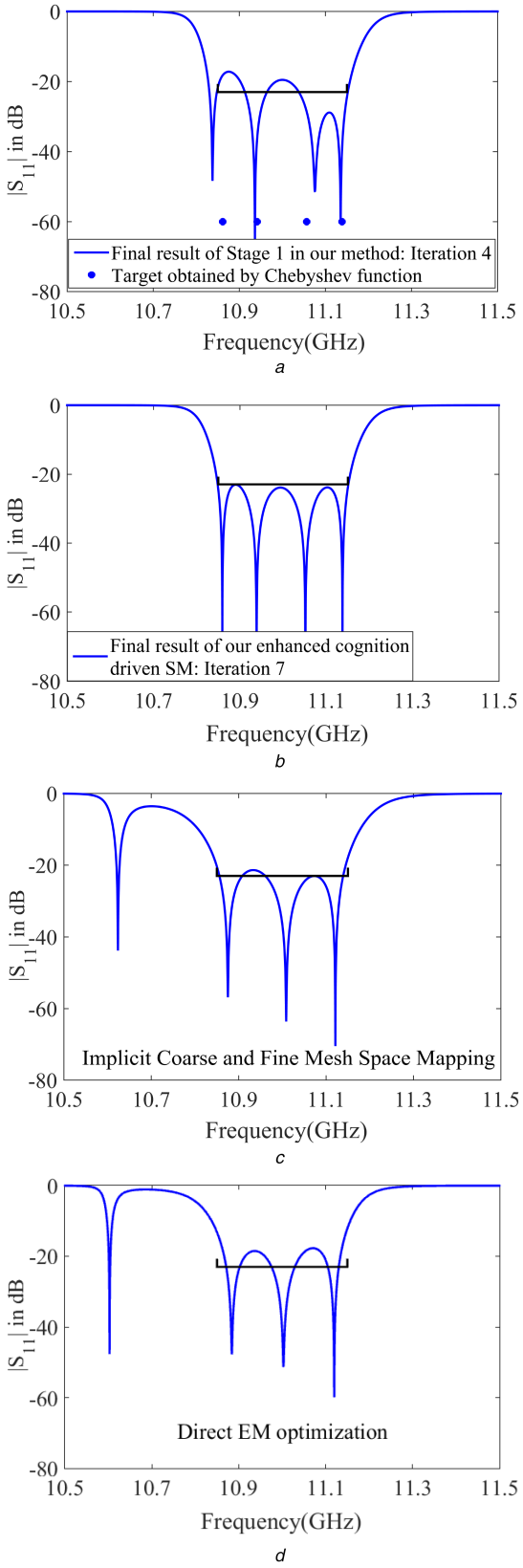

Fig. 6 *Comparison of the results for three different optimisation methods for the four-pole waveguide filter with an incorrect number of feature frequency parameters at the starting point in Case II*

(a) Using our enhanced cognition-driven SM method, all of the feature frequency parameters move to the passband according to the target obtained by the Chebyshev filter function after the first stage, ***(b)*** Using our enhanced cognition-driven SM method, a good equal-ripple response is obtained after seven iterations, and our method can avoid being trapped in a local minimum, ***(c)*** Using the implicit coarse and fine mesh SM method, the optimisation process falls into a local minimum, ***(d)*** Using direct EM optimisation, the optimisation process falls into a local minimum

Table 2 Comparisons of four optimisation methods for the four-pole waveguide filter example with incorrect number of feature frequency parameters at the initial filter in Case II

Optimisation method	Direct EM optimisation (existing technique)	Coarse/ fine mesh SM (existing technique)	Cognition-driven SM (existing technique)	Enhanced cognition SM (proposed technique)
no. of iterations	600	3	—	$1^{a} + 7$
fine model evaluation time	600 × 4 min	4 × 4 min	—	$(1^{a} + 8 + 6^{b})$ × 6 min
training time	—	2 × 1 h	—	8 × 1 min
design optimisation time	—	4 × 1 h	—	8 × 1 min
total time	40 h	5 h 16 min	—	1 h 46 min
final value of objective function	152.15 (being trapped in local minimum)	28.27 (being trapped in local minimum)	cannot work well[c]	−0.02

[a]The iteration to split the ambiguous feature.

[b]The number of EM simulations, which are not accepted during the trust region adjustment.

[c]The existing cognition-driven SM cannot proceed because of the incorrect number of feature frequency parameters.

Table 3 Comparisons of four optimisation methods for the iris coupled cavity filter example with correct number of feature frequency parameters at the initial filter in Case I

Optimisation method	Direct EM optimisation (existing technique)	Coarse/ fine mesh SM (existing technique)	Cognition-driven SM (existing technique)	Enhanced cognition SM (proposed technique)
no. of iterations	300	3	12	9
fine model evaluation time	300 × 30 min	4 × 30 min	$(13 + 3^{a})$ × 40 min	$(10 + 2^{a})$ × 40 min
training time	—	2 × 5 h	12 × 1 min	9 × 1 min
design optimisation time	—	3 × 4 h	12 × 1 min	9 × 1 min
total time	150 h	24 h	11 h	8.5 h
final value of objective function	239.77 (being trapped in local minimum)	232.61 (being trapped in local minimum)	−0.17	−0.04

[a]The number of EM simulations, which are not accepted during the trust region adjustment.

$\boldsymbol{x}^{(0)} =$ [113.410 56.322 53.416 58.406 43.645 49.885 50.126]^{T} (all values in mm). The response curve of this starting point has only five feature frequency parameters as shown in Fig. 7*a*. This incorrect number of feature frequency parameters will give the target defined in (1) incomplete information, which makes it difficult for the existing cognition-driven SM [3] to proceed in the first stage. Therefore, our proposed technique is needed. Our algorithm can firstly find that the second feature frequency parameter is the ambiguous feature. The sharpness parameters of the five feature frequency points are 1449.950, 0.512, 1590.920, 1505.244, and 1172.158, respectively. We can find that the sharpness parameter of the ambiguous feature (the second one) is obviously smaller than that of non-ambiguous feature frequency

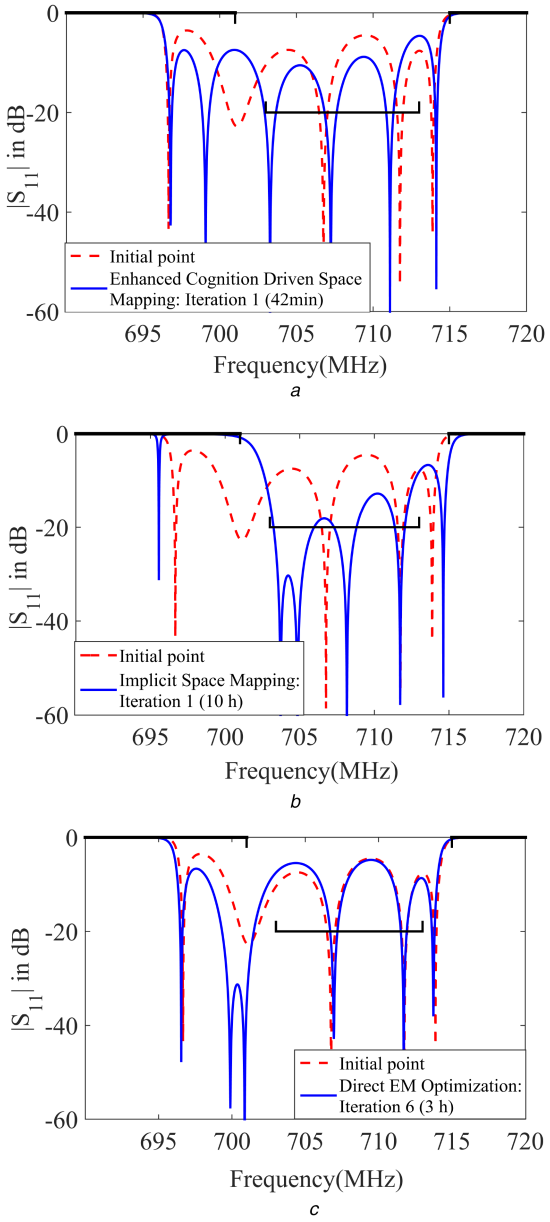

Fig. 7 *Different methods to split the ambiguous feature for the iris coupled cavity filter in Case II*

(a) Our enhanced cognition SM method takes one iteration (42 min), ***(b)*** Implicit coarse and fine mesh SM takes one iteration (10 h), ***(c)*** Direct EM optimisation takes six iterations (3 h)

parameters. After finding the ambiguous feature, we use our technique to split the ambiguous feature. The number of feature frequency parameters is increased from five to six after splitting the ambiguous feature using one iteration (42 min). The responses of the initial point and the first iteration are shown in Fig. 7*a*. From the figure, we can find that our algorithm can split the ambiguous feature while the locations of non-ambiguous feature frequency parameters are almost unchanged.

For comparison purposes, we use implicit coarse and fine mesh SM and direct EM optimisation to optimise this filter until the ambiguous feature is split. Fig. 7*b* shows that the implicit coarse and fine mesh SM method can split the ambiguous feature into one SM iteration, and takes more than 10 h to finish one SM iteration. The computation time is mostly spent on coarse mesh EM optimisations. Fig. 7*c* shows that direct EM optimisation achieves our goal to split the ambiguous feature into six iterations and that takes nearly 3 h. We can find that our enhanced technique uses the shortest time to split the ambiguous feature to produce a good result with the correct number of feature frequency parameters.

After obtaining the solution with enough feature frequency parameters, we use our enhanced technique to continue the

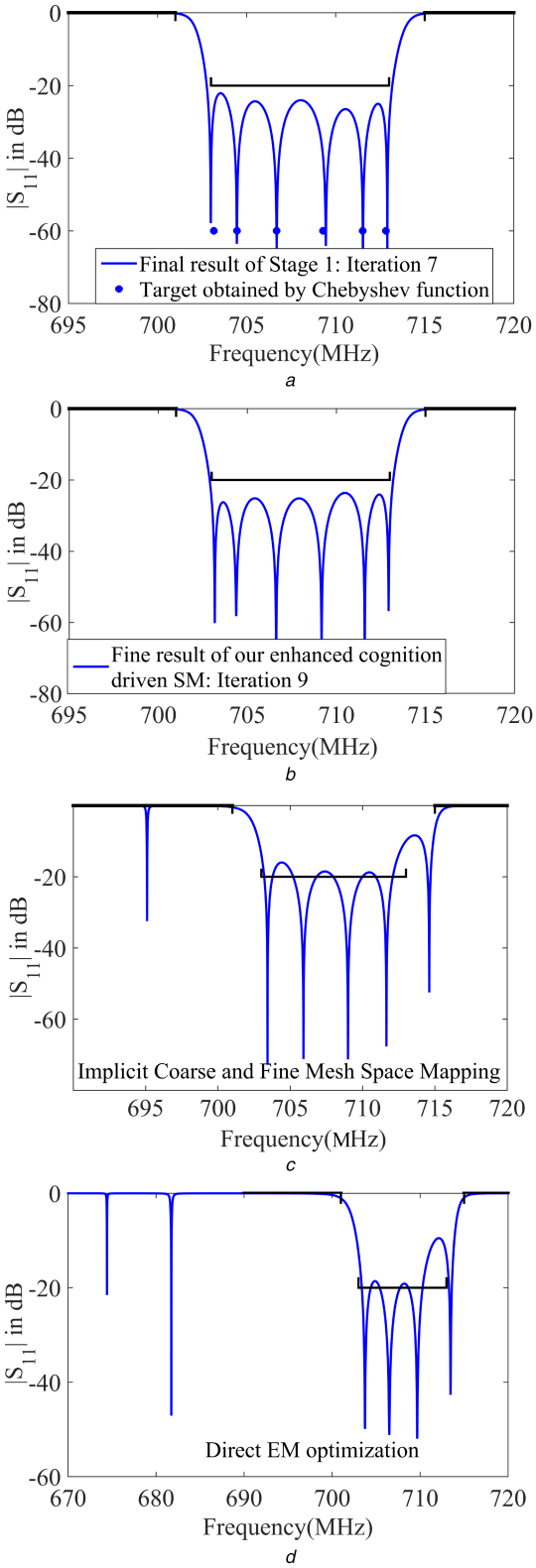

Fig. 8 *Comparison of the results for three different optimisation methods for the iris coupled cavity filter example with an incorrect number of feature frequency parameters at the initial filter in Case II*

(a) Using our enhanced cognition-driven SM method, all of the feature frequency parameters move to the passband according to the target obtained by the Chebyshev filter function after the first stage, ***(b)*** Using our enhanced cognition-driven SM method, a good equal-ripple response is obtained after nine iterations, and our method can avoid being trapped in a local minimum, ***(c)*** Using the implicit coarse and fine mesh SM, the optimisation process falls into a local minimum, ***(d)*** Using the direct EM optimisation, the optimisation process falls into a local minimum

Table 4 Comparisons of four optimisation methods for the iris coupled cavity filter example with incorrect number of feature frequency parameters at the initial filter in Case II

Optimisation method	Direct EM optimisation (existing technique)	Coarse/ fine mesh SM (existing technique)	Cognition-driven SM (existing technique)	Enhanced cognition SM (proposed technique)
no. of iterations	200	3	—	1[a] + 9
fine model evaluation time	200 × 30 min	4 × 30 min	—	(1[a] + 9 + 7[b]) × 40 min
training time	—	2 × 5 h	—	10 × 1 min
design optimisation time	—	3 × 4 h	—	10 × 1 min
total time	100 h	22 h 16 min	—	12 h
final value of objective function	151.60 (being trapped in local minimum)	114.82 (being trapped in local minimum)	can't work well[c]	−0.11

[a]The iteration to split the ambiguous feature.

[b]The number of EM simulations, which are not accepted the during trust region adjustment.

[c]The existing cognition-driven SM cannot proceed because of the incorrect number of feature frequency parameters.

optimisation. The optimal solution $\boldsymbol{x}^{(9)} = [120.068 \quad 52.409 \quad 45.445 \quad 48.550 \quad 41.715 \quad 50.143 \quad 50.351]^{\mathrm{T}}$ (all values in mm) is obtained after nine iterations, which include seven iterations in Stage 1 and two iterations in Stage 2. Fig. 8*a* shows the final result for Stage 1. We can find that after Stage 1 the result is very close to an equal-ripple Chebyshev filter response. Obviously, the Chebyshev target for Stage 1 is much better than the previous uniformly distributed target. The final result of our enhanced technique is shown in Fig. 8*b*. All the feature space objective functions [3] are shown in Fig. 3*c*.

For comparison purposes, we use implicit coarse and fine mesh SM and the direct EM optimisation to optimise this filter with the same initial point and the same specifications as those shown in Fig. 7*a*. The results are shown in Figs. 8*c* and *d*. The results in Fig. 8 and Table 4 show that both implicit coarse and fine mesh SM and the direct EM optimisation fall into local minima. Our enhanced method can solve the initial point with an incorrect number of feature frequency parameters, increase the optimisation efficiency and find a better result within less time.

5 Conclusion

Our cognition-driven formation of SM is an effective method for equal-ripple optimisation of microwave filters. This technique increases the optimisation efficiency and has the ability to avoid being trapped in a local minimum. The existing cognition-driven SM assumes that the number of feature parameters is correct, and uses an equally divided passband specification as the target in the first stage. This study proposes an enhanced technique which can run successfully even if the number of feature frequency parameters is incorrect in the initial design. Additionally, our proposed technique incorporates filter design knowledge of the Chebyshev filter function into cognition-driven SM. To obtain the target for the first stage, we use feature frequency parameters of the Chebyshev filter function response curve to replace the equally divided passband specifications. With this new target, our enhanced cognition-driven SM can obtain a good result in the first stage and give a better starting point for the second stage. Our enhanced cognition-driven SM method can increase the optimisation efficiency and has the ability to avoid being trapped in a local minimum over the existing coarse and fine mesh SM and

direct EM optimisation methods. This enhanced technique is well suited to the EM-based design of Chebyshev- and elliptic-type filters and is more robust than the previous cognition-driven SM method.

6 Acknowledgments

This work was supported in part by the Natural Sciences and Engineering Research Council of Canada under Grants RGPIN-2017-06420, RGPIN7239-11 and Bandler Coporation.

7 References

[1] Bandler, J.W., Biernacki, R.M., Chen, S.H., *et al.*: 'Space mapping technique for electromagnetic optimization', *IEEE Trans. Microw. Theory Tech.*, 1994, **42**, (12), pp. 2536–2544

[2] Rayas-Sanchez, J.E.: 'Power in simplicity with ASM: tracing the aggressive space mapping algorithm over two decades of development and engineering applications', *IEEE Microw. Mag.*, 2016, **17**, (4), pp. 64–76

[3] Zhang, C., Feng, F., Gongal-Reddy, V., *et al.*: 'Cognition-driven formulation of space mapping for equal-ripple optimization of microwave filters', *IEEE Trans. Microw. Theory Tech.*, 2015, **63**, (7), pp. 2154–2165

[4] Zhang, L., Aaen, P.H., Wood, J.: 'Portable space mapping for efficient statistical modeling of passive components', *IEEE Trans. Microw. Theory Tech.*, 2012, **60**, (3), pp. 441–450

[5] Ayed, R.B., Gong, J., Brisset, S., *et al.*: 'Three-level output space mapping strategy for electromagnetic design optimization', *IEEE Trans. Magn.*, 2012, **48**, (2), pp. 671–674

[6] Koziel, S., Meng, J., Bandler, J.W., *et al.*: 'Accelerated microwave design optimization with tuning space mapping', *IEEE Trans. Microw. Theory Tech.*, 2009, **57**, (2), pp. 383–394

[7] Leszczynska, N., Szydlowski, L., Mrozowski, M.: 'Zero-pole space mapping for CAD of filters', *IEEE Microw. Wirel. Compon. Lett.*, 2014, **24**, (9), pp. 581–583

[8] Feng, F., Zhang, C., Gongal-Reddy, V., *et al.*: 'Parallel space-mapping approach to EM optimization', *IEEE Trans. Microw. Theory Tech.*, 2014, **62**, (5), pp. 1135–1148

[9] Zhu, L., Zhang, Q.J., Liu, K., *et al.*: 'A novel dynamic neuro-space mapping approach for nonlinear microwave device modeling', *IEEE Microw. Wirel. Compon. Lett.*, 2016, **26**, (2), pp. 131–133

[10] Morro, J.V., Soto, P., Esteban, H., *et al.*: 'Fast automated design of waveguide filters using aggressive space mapping with a new segmentation strategy and a hybrid optimization algorithm', *IEEE Trans. Microw. Theory Tech.*, 2005, **53**, (4), pp. 1130–1142

[11] Koziel, S., Ogurtsov, S.: 'Model management for cost-efficient surrogate-based optimization of antennas using variable-fidelity electromagnetic simulations', *IET Microw. Antennas Propag.*, 2012, **6**, (15), pp. 1643–1650

[12] Koziel, S., Ogurtsov, S., Bandler, J.W., *et al.*: 'Reliable space-mapping optimization integrated with EM-based adjoint sensitivities', *IEEE Trans. Microw. Theory Tech.*, 2013, **61**, (10), pp. 3493–3502

[13] Ichige, K., Takeuchi, Y., Miyamoto, K., *et al.*: 'Successive optimization of zeros of reflection characteristics for automated microwave filter tuning'. IEEE MTT-S Int. Microwave Symp. Digest, Baltimore, USA, June 2011

[14] Koziel, S., Bekasiewicz, A.: 'Fast simulation-driven feature-based design optimization of compact dual-band microstrip branch-line coupler', *Int. J. RF Microw. Comput.-Aided Eng.*, 2016, **26**, (1), pp. 13–20

[15] Koziel, S., Bandler, J.W.: 'Rapid yield estimation and optimization for microwave structures exploiting feature-based statistical analysis', *IEEE Trans. Microw. Theory Tech.*, 2015, **63**, (1), pp. 107–114

[16] Koziel, S., Bandler, J.W.: 'Reliable microwave modeling by means of variable-fidelity response features', *IEEE Trans. Microw. Theory Tech.*, 2015, **63**, (12), pp. 4247–4254

[17] Alexandrov, N.M., Dennis, J.E., Lewis, R.M., *et al.*: 'A trust region framework for managing use of approximation models in optimization', *Struct. Multidiscip. Optim.*, 1998, **15**, (1), pp. 16–23

[18] Koziel, S., Bandler, J.W., Cheng, Q.S.: 'Robust trust-region space-mapping algorithms for microwave design optimization', *IEEE Trans. Microw. Theory Tech.*, 2010, **58**, (8), pp. 2166–2174

[19] Cameron, R.J., Kudsia, C.M., Mansour, R.T.: '*Microwave filters for communication systems: fundamentals, design, and applications*' (John Wiley & Sons Inc., Hoboken, New Jersey, 2007)